

Extreme Metal Carbonyl Back Bonding in Cyclopentadienylthorium Carbonyls Generates Bridging C_2O_2 Ligands by Carbonyl Coupling

Huidong Li,^{†,‡} Hao Feng,^{*,†,‡} Weiguo Sun,^{†,‡} R. Bruce King,^{*,§} and Henry F. Schaefer, III[§]

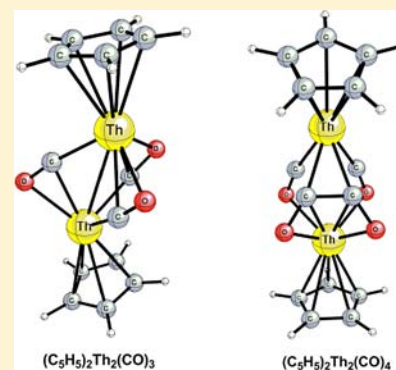
[†]School of Physics and Chemistry, Research Center for Advanced Computation, Xihua University, Chengdu, China 610039

[‡]Institute of Atomic and Molecular Physics, Sichuan University, Chengdu, Sichuan 610065, China

[§]Department of Chemistry and Center for Computational Quantum Chemistry, University of Georgia, Athens, Georgia 30602, United States

S Supporting Information

ABSTRACT: Laboratory studies of the interaction of carbon monoxide with organoactinides result in the formation of isolable complexes such as Cp_3UCO derivatives (Cp = cyclopentadienyl) as well as coupling reactions to give derivatives of the oligomeric anions $C_nO_n^{2-}$ ($n = 2, 3, 4$). To gain some insight into actinide carbonyl chemistry, binuclear cyclopentadienylthorium carbonyls $Cp_2Th_2(CO)_n$ ($n = 2$ to 5) as model compounds have been investigated using density functional theory. The most favorable such structures in terms of energy and thermochemistry are the tricarbonyl $Cp_2Th_2(\eta^2-\mu-CO)_3$ having three four-electron donor bridging carbonyl groups and the tetracarbonyl $Cp_2Th_2(\eta^4-\mu-C_2O_2)(\eta^2-\mu-CO)_2$ having not only two four-electron donor bridging carbonyl groups but also a bridging ethynediolate ligand formed by coupling two CO groups through C–C bond formation. The bridging infrared $\nu(CO)$ frequencies ranging from 1140 to 1560 cm^{-1} in these $Cp_2Th_2(CO)_n$ ($n = 3, 4$) derivatives indicate extremely strong Th→CO back bonding in these structures, corresponding to formally dianionic CO^{2-} and $C_2O_2^{2-}$ ligands and the favorable +4 thorium oxidation state. A characteristic of the $Cp_2Th_2(\eta^2-\mu-CO)_3$ and $Cp_2Th_2(\eta^4-\mu-C_2O_2)(\eta^2-\mu-CO)_2$ structures is their ability to add terminal CO groups, preferably to the thorium atom bonded to the fewest oxygen atoms. These terminal CO groups exhibit $\nu(CO)$ frequencies in a similar range as terminal CO groups in d-block metal carbonyls. However, these terminal CO groups are relatively weakly bonded to the thorium atoms as indicated by predicted CO dissociation energies of 14 kcal/mol for $Cp_2Th_2(CO)_5$. Two low energy structures for the dicarbonyl $Cp_2Th_2(CO)_2$ are found with two separate four-electron donor bridging CO groups and relatively short Th–Th distances of 3.3 to 3.4 Å suggesting formal single bonds and +3 thorium formal oxidation states. However, a QTAIM analysis of this formal Th–Th bond does not reveal a bond critical point thus suggesting a multicenter bonding model involving the bridging CO groups.



1. INTRODUCTION

Metal carbonyl chemistry dates back to the 19th century with the synthesis of $[Pt(CO)Cl_2]_2$ in 1868.¹ The first binary metal carbonyl to be synthesized was $Ni(CO)_4$, reported in 1890.² During the next half century a number of other stable binary metal carbonyls were discovered including $Fe(CO)_5$, $Fe_2(CO)_9$, $Fe_3(CO)_{12}$, $Co_2(CO)_8$, and $M(CO)_6$ ($M = Cr, Mo, \text{ and } W$).³ These are all commercially available and have become key intermediates for the synthesis of a variety of organometallic compounds. They are also important catalyst precursors as well as agents for metal deposition.

All of these stable homoleptic metal carbonyls involve d-block transition metals. They owe their stability to $d\pi \rightarrow p\pi^*$ back bonding from filled metal d orbitals into empty π^* antibonding orbitals of the CO ligands (Figure 1).⁴ The nature of this back-bonding has been studied in detail by Frenking and collaborators^{5,6} on the simple octahedral homoleptic hexacarbonyls of the third row transition metals using density functional theory. Such back bonding concurrently removes metal electron density from the metal atom and decreases the

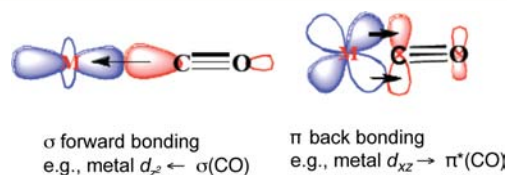


Figure 1. Forward and back bonding of the CO ligand to a metal atom.

effective C–O bond order of the CO group. The effects of such back-bonding in terms of the formal metal–carbon and carbon–oxygen bond orders can simply be represented in a series of resonance structures (Figure 2). The typically intense $\nu(CO)$ frequencies reflecting such changes in the effective C–O bond order are very sensitive to the extent of such back bonding. For terminal CO groups in stable neutral carbonyls of

Received: November 29, 2012

Published: May 30, 2013

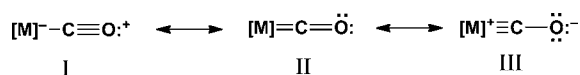


Figure 2. Resonance structures illustrating the effect of back bonding on removing negative charge from the metal atom. The designation [M] refers to the metal atom with all associated ligands other than the CO group in question.

the d-block metals, the $\nu(\text{CO})$ frequencies are lower than those in free CO but only by 100 to 200 cm^{-1} . For bridging CO groups in such metal carbonyls, where increased back-bonding is expected from interaction of the CO group with two metals rather than a single metal, the $\nu(\text{CO})$ frequencies are $\sim 100 \text{ cm}^{-1}$ below those for the terminal CO groups but still less than the $\nu(\text{CO})$ frequencies for the simple $\text{C}=\text{O}$ double bonded CO groups in aldehydes and ketones. Thus a simplified but useful model of the M-CO bonding in such metal carbonyls is a resonance hybrid between structures I and II (Figure 2).

The removal of electron density from the metal atom by back bonding to CO groups has the effect of stabilizing low formal metal oxidation states. The most dramatic example of this behavior lies in the formally zerovalent chromium derivative $\text{Cr}(\text{CO})_6$, which is even stable to steam-distillation in air, contrasting with the air-sensitivity of Cr(II) derivatives of more normal ligands such as chromium(II) acetate, $\text{Cr}_2(\text{O}_2\text{CCH}_3)_4$.

The assignment of the zerovalent formal oxidation state to the homoleptic metal carbonyls $\text{M}(\text{CO})_n$ assumes that the CO moieties are neutral ligands. However, the $d\pi \rightarrow p\pi^*$ back bonding of a metal to a CO ligand can also be considered as a redox process in which the metal is oxidized by an indeterminate amount and the CO ligand is correspondingly reduced by an indeterminate amount. In addition to the availability of metal orbitals the reducing power of the metal atom can determine the extent of back bonding. For the d-block transition metals this effect is manifested in the decreasing $\nu(\text{CO})$ frequencies in the isoelectronic series of the octahedral first row transition metal carbonyls $\text{Fe}(\text{CO})_6^{2+} \rightarrow \text{Mn}(\text{CO})_6^{+} \rightarrow \text{Cr}(\text{CO})_6 \rightarrow \text{V}(\text{CO})_6^{-} \rightarrow \text{Ti}(\text{CO})_6^{2-}$ as the reducing power of the metal atom is increased by lowering the formal oxidation state.⁷ A similar effect has been studied in more detail for the analogous octahedral third row transition metal hexacarbonyls.^{5,6}

The dearth of metal carbonyl derivatives of the f-block metals, particularly the actinides, contrasts with the abundance of stable metal carbonyls of the d-block metals. In the early days of metal carbonyl chemistry, before the special position of the actinides in the Periodic Table was recognized, uranium was placed in the same group as chromium, molybdenum, and tungsten. This stimulated efforts to synthesize a stable $\text{U}(\text{CO})_6$ analogous to the very stable metal carbonyls $\text{M}(\text{CO})_6$ ($\text{M} = \text{Cr}, \text{Mo}, \text{W}$) using analogous synthetic methods. Such efforts always failed and, as is typical with such experimental failures, are only reported in obscure journals.⁸

We now recognize that uranium does not lie under tungsten in the Periodic Table and thus are not surprised that the early efforts to synthesize $\text{U}(\text{CO})_6$ led to failure. However, the f-block metals, including particularly the actinides, have suitable d and f orbitals in terms of symmetry to participate in metal $d\pi \rightarrow p\pi^*$ and $f\pi \rightarrow p\pi^*$ back bonding. Therefore, the dearth of stable carbonyls of the f-block metals must arise from features of their chemistry other than the lack of suitable metal orbitals for back bonding.

In more recent years a few carbonyl derivatives of f-block metals, particularly uranium, have been discovered. The first such species to be isolated and structurally characterized was the uranium derivative $(\text{Me}_4\text{C}_5\text{H})_3\text{U}(\text{CO})$.^{9,10} The $\nu(\text{CO})$ frequency of 1880 cm^{-1} found for this species as well as the geometry of the CO ligand are similar to those in cyclopentadienylmetal carbonyls of the d-block metals.

Binary carbonyl derivatives of the f-block metals appear to exist mainly in the gas phase or in low temperature matrices. Thus enhanced abundance in the mass spectra was found for $\text{U}(\text{CO})_8^{+}$ as well as for the uranyl carbonyl $\text{UO}_2(\text{CO})_3^{+}$ in a very recent study.¹¹ The thorium carbonyls $\text{Th}(\text{CO})_n$ ($n = 1$ to 6)^{12,13} and uranium carbonyls $\text{U}(\text{CO})_n$ ($n = 1, 2, 6$)¹⁴ have been obtained by reactions of laser-ablated metal atoms with CO and characterized by their $\nu(\text{CO})$ frequencies in low-temperature matrices. The $\nu(\text{CO})$ frequencies of lanthanide^{15,16} and actinide^{17,18} carbonyl compounds have attracted much attention in recent years. Sheline and Slater¹⁹ have systematically reviewed the infrared $\nu(\text{CO})$ frequencies of lanthanide and actinide carbonyl compounds.

Even though stable actinide carbonyl derivatives are rare, carbon monoxide undergoes a variety of interesting reductive coupling reactions with organoactinide systems.^{20,21} Such reactions have proven useful for the synthesis of oxocarbon anions. For example the reaction of CO with uranium(III) sandwich compounds of the type $(\eta^5\text{-Me}_5\text{C}_5)\text{U}(\eta^8\text{-C}_8\text{H}_6\{\text{SiR}_3\}_2)$ leads to reductive coupling to give ethynediolate ($\text{C}_2\text{O}_2^{2-}$), deltate ($\text{C}_3\text{O}_3^{2-}$), and squarate ($\text{C}_4\text{O}_4^{2-}$) derivatives of uranium(IV).²²⁻²⁷ Mechanistic and theoretical²⁸ studies of these uranium-based CO reductive coupling systems have been reported. A driving force behind these reactions appears to be the oxidation of uranium(III) in the initial organometallic to uranium(IV) in the CO reductive coupling product. Such a uranium oxidation from the +3 oxidation state to the +4 oxidation state can be considered to be an extreme example of back bonding of a metal atom to a CO ligand. This metal oxidation reduces the CO ligand to an anionic species readily susceptible to coupling reactions giving ethynediolate, deltate, squarate, and so forth. Because of the accessibility of the U(III) oxidation state relative to the Th(III) oxidation state, all of the reported actinide CO coupling chemistry involves uranium rather than the other generally available actinide thorium.

Experimental work during the past half century suggests that binary actinide carbonyls such as $\text{An}(\text{CO})_n$ are not likely to exist as stable molecules under normal laboratory conditions. However, the stability of selected Cp_3UCO ($\text{Cp} = \text{cyclopentadienyl}$ ligand) derivatives^{9,10} suggests the possibility of significant cyclopentadienylactinide carbonyl chemistry. To explore the possibilities in this area we have used density functional theory to investigate the structures and thermochemistry of $\text{Cp}_2\text{Th}_2(\text{CO})_n$ ($n = 5, 4, 3, 2$) derivatives. Thorium was chosen rather than uranium for this initial study because of the simpler chemistry of thorium involving almost entirely the +4 formal oxidation state and species with singlet spin states. Using the thorium derivatives for this initial theoretical study also provides a comparison with the previously studied²⁹ titanium analogues $\text{Cp}_2\text{Ti}_2(\text{CO})_n$. Both the d-block metal titanium and the f-block metal thorium are located four elements in the Periodic Table after a noble gas, namely, argon and radon, respectively. Thus this study provides an opportunity to compare the potentially experimentally accessible chemistry of otherwise similar d-block and f-block metals, namely, titanium and thorium, respectively.

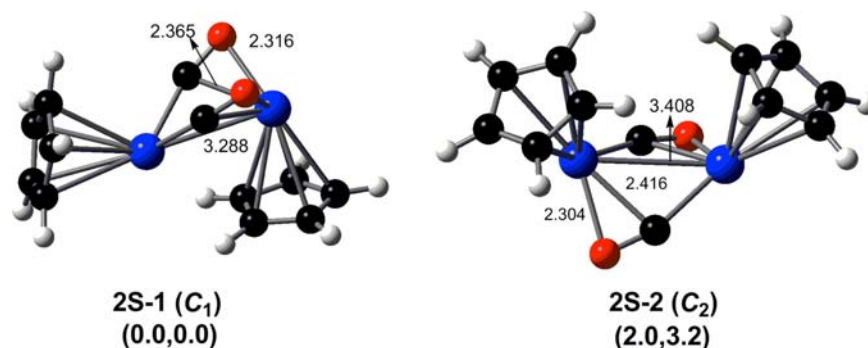


Figure 3. Two optimized $\text{Cp}_2\text{Th}_2(\text{CO})_2$ structures. Figures 3 to 6 show the optimized distances in Å by the BP86 method. The numbers in parentheses are the relative energies (ΔE in kcal/mol) predicted by BP86 and M06-L methods.

To maximize the results relative to the computational resources we have used the unsubstituted cyclopentadienyl ligand $\eta^5\text{-C}_5\text{H}_5$ for these studies. However, we realize that to achieve experimentally any of the structures predicted from this research, suitably substituted cyclopentadienyl ligands will probably be necessary. This has already been demonstrated in the published work^{9,10} leading to the synthesis of stable Cp_3UCO derivatives. The reductive carbonylation of suitably chosen cyclopentadienylthorium halides using strong reducing agents such as alkali metals provide possible synthetic routes to the compounds discussed in this paper.

2. THEORETICAL METHODS

Electron correlation effects have been included to some degree using density functional theory (DFT) methods, which have evolved as a practical and effective computational tool for organometallic compounds^{30–36} including actinide derivatives.^{37–39} Two differently constructed DFT functionals, namely the BP86 and the M06-L functionals, were used in the present study. The BP86 method combines Becke's 1988 exchange functional (B) with Perdew's 1986 gradient-corrected correlation functional method (P86).^{40,41} This method has been shown to be effective for the study of transition metal and actinide complexes.^{42,43} The second functional used in this work is a hybrid *meta*-GGA DFT method, M06-L, developed by Truhlar's group.^{44,45} The studies in Truhlar's group suggest that M06-L is one of the best functionals for the study of organometallic and inorganic thermochemistry, and perhaps the best current functional for transition metal energetics. When these two conceptually different DFT methods agree, confident predictions can be made.

Scalar relativistic effects were incorporated by using an (14s13p10d8f6g/10s9p5d4f3g) effective core potential (ECP) basis set with 60 core electrons for the thorium atoms.⁴⁶ The Ahlrichs TZVP valence triple- ζ basis sets with polarization functions were used for all of the other atoms.^{47,48}

The geometries of all structures were fully optimized using both functionals with the grid (120, 974) for evaluating integrals numerically in the Gaussian09 program.⁴⁹ In all of the computations no constraints were imposed on the starting geometry. Harmonic vibrational frequencies and infrared intensities were determined at the same levels. The tight designation is the default for the energy convergence. In the search for minima, low-magnitude imaginary vibrational frequencies may be suspect, because the numerical integration procedures used in existing DFT methods have significant limitations.⁵⁰ All of the final optimized structures reported in this paper have only real vibrational frequencies unless otherwise indicated.

3. RESULTS

Extensive searches for the global and local minimum $\text{Cp}_2\text{Th}_2(\text{CO})_n$ structures ($n = 2$ to 5) were made using the BP86 and M06-L methods. A variety of different geometries

with different numbers of terminal CO groups attached on each Th atom were used as starting structures for the optimization. However, most of the low energy optimized structures have two, three, or four bridging CO groups. To reduce the length of this report some of the high-energy structures of questionable chemical significance, especially many triplet structures, are excluded. Therefore, only the lowest energy chemically important structures are discussed in the present paper.

3.1. $\text{Cp}_2\text{Th}_2(\text{CO})_2$ Structures. Two low-lying singlet $\text{Cp}_2\text{Th}_2(\text{CO})_2$ structures were found (Figure 3 and Supporting Information, Table S35). Triplet $\text{Cp}_2\text{Th}_2(\text{CO})_2$ structures were found to be significantly higher in energy (>17 kcal/mol) than the singlet structures and thus are not discussed in this paper. For the lowest energy structure **2S-1**, the BP86 method predicts C_s symmetry, whereas the M06-L method predicts C_1 symmetry. In **2S-1** the thorium atoms are bridged by a pair of four-electron donor $\eta^2\text{-}\mu\text{-CO}$ carbonyl groups oriented in the same direction with one thorium atom bonded to both carbon atoms and the other thorium atom bonded to both oxygen atoms. The predicted Th–Th distance for **2S-1** of is 3.288 Å (BP86) or 3.289 Å (M06-L).

The other predicted $\text{Cp}_2\text{Th}_2(\text{CO})_2$ structure is the singlet C_2 structure **2S-2**, lying 2.0 kcal/mol (BP86) or 3.2 kcal/mol (M06-L) above **2S-1** (Figure 3 and Supporting Information, Table S35). Structure **2S-2** differs from **2S-1** in having the two bridging $\eta^2\text{-}\mu\text{-CO}$ groups oriented in opposite directions. The predicted Th–Th distance is 3.408 Å (BP86) or 3.350 Å (M06-L) in **2S-2**. These short Th–Th distances in both $\text{Cp}_2\text{Th}_2(\text{CO})_2$ structures **2S-1** and **2S-2** suggest a strong direct Th–Th bond. If the bridging CO ligands are formally dianions, then the formal thorium oxidation state in **2S-1** and **2S-2** is +3, suggesting the possibility of a Th–Th single bond in these structures.

3.2. $\text{Cp}_2\text{Th}_2(\text{CO})_3$ Structures. Two low-lying structures are predicted for $\text{Cp}_2\text{Th}_2(\text{CO})_3$, namely **3S-1** and **3S-2** (Supporting Information, Table S32 and Figure 4). The global minimum structure **3S-1** is predicted by the much finer grid (400, 974) to be a C_s (BP86) or C_1 (M06-L) singlet structure with three bridging four-electron donor $\eta^2\text{-}\mu\text{-CO}$ groups. Two of these bridging CO groups are oriented in one direction and the third such CO group in the other direction. Thus one thorium atom in **3S-1** is bonded to the carbon atoms of two of the CO groups and the oxygen atom of the third CO group. The second thorium atom in **3S-1** is bonded to the oxygen atoms of two of the CO groups and the carbon atom of the third CO group. The two four-electron donor bridging CO groups oriented in the same direction can be characterized by bonding Th–O

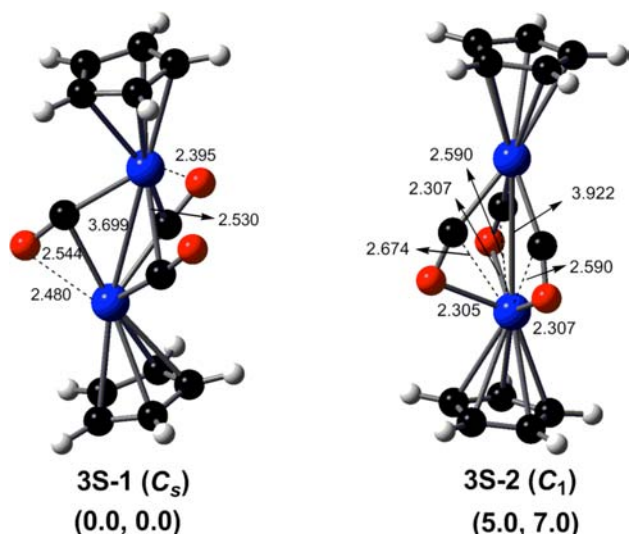


Figure 4. Two optimized $\text{Cp}_2\text{Th}_2(\text{CO})_3$ structures.

distances of 2.395 Å (BP86) and 2.407 Å (M06-L). The third four-electron donor bridging CO group is likewise indicated by a slightly longer, but still bonding Th–O distance of 2.480 Å (BP86) or 2.498 Å (M06-L). The Th⋯Th distance is 3.699 Å (BP86) or 3.681 Å (M06-L) in 3S-1.

The second $\text{Cp}_2\text{Th}_2(\text{CO})_3$ structure 3S-2 is similar to 3S-1 in having the Th_2 unit bridged by three four-electron donor η^2 - μ -CO groups (Figure 4 and Supporting Information, Table S32). However, in 3S-2 all three bridging CO groups are oriented in the same direction so that all three carbon atoms are bonded to one of the thorium atoms and all three oxygen atoms are bonded to the other thorium atom. Structure 3S-2 is predicted to be less favorable than 3S-1, lying 5.0 kcal/mol (BP86) or 7.0 kcal/mol (M06-L) in energy above 3S-1. The Th–Th distance of 3.922 Å (BP86) or 3.879 Å (M06-L) in 3S-2 is ~ 0.2 Å longer than that in 3S-1.

3.3. $\text{Cp}_2\text{Th}_2(\text{CO})_4$ Structures. Four low-lying structures are predicted for $\text{Cp}_2\text{Th}_2(\text{CO})_4$ (Figure 5 and Supporting Information, Table S33). In the three lowest energy of these $\text{Cp}_2\text{Th}_2(\text{CO})_4$ structures one thorium atom is linked to all of the carbon atoms and the other thorium atom is linked to all of the oxygen atoms. The lowest energy $\text{Cp}_2\text{Th}_2(\text{CO})_4$ structure is the C_1 singlet 4S-1 with four bridging carbonyls. In 4S-1, two of the four bridging carbonyl groups are coupled to form a C_2O_2 unit with a C–C bond of length 1.480 Å (BP86) or 1.484 Å (M06-L). Such a η^4 - μ - C_2O_2 ligand may be regarded as a six-electron donor to the pair of thorium atoms. The other two carbonyl groups remain as discrete uncoupled CO ligands corresponding to four-electron donor bridging η^2 - μ -CO groups. The long Th⋯Th distance of 4.061 Å (BP86) or 3.926 Å (M06-L) in 4S-1 suggests a lack of conventional metal–metal bonding.

The second $\text{Cp}_2\text{Th}_2(\text{CO})_4$ structure is the C_s singlet 4S-2 lying 2.4 kcal/mol (BP86) or 3.5 kcal/mol (M06-L) above the global minimum structure 4S-1 (Figure 5 and Supporting Information, Table S33). The coordination mode of the carbonyl groups in 4S-2 is very similar to that in the global minimum structure 4S-1 except for the presence of two pairs of coupled carbonyl groups so that structure 4S-2 can be considered as $\text{Cp}_2\text{Th}_2(\eta^4\text{-}\mu\text{-C}_2\text{O}_2)_2$. However, the C–C distances of 1.630 Å (BP86) or 1.670 Å (M06-L) joining these pairs of coupled carbonyl groups are significantly longer

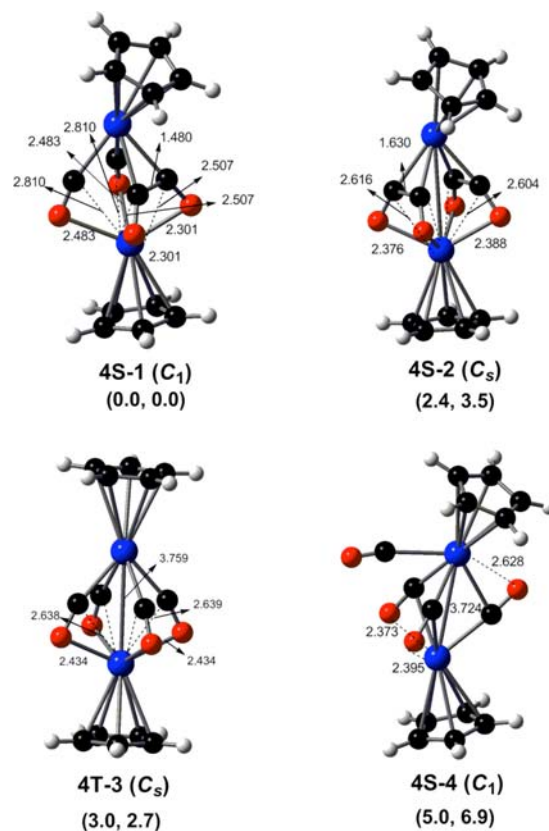


Figure 5. Four optimized $\text{Cp}_2\text{Th}_2(\text{CO})_4$ structures.

than the 1.480 Å distance in 4S-1. Two small imaginary vibrational frequencies of $60i$ and $8i$ cm^{-1} are predicted by the M06-L method for 4S-2. However, the BP86 method predicts all real vibrational frequencies. Following the normal mode of the largest imaginary frequency in 4S-2 leads to 4S-1. The long Th⋯Th distance of 4.030 Å (BP86) or 3.977 Å (M06-L) in 4S-2 is similar to that predicted for the global minimum structure 4S-1 and likewise suggests the lack of a formal thorium–thorium bond.

The third $\text{Cp}_2\text{Th}_2(\text{CO})_4$ structure predicted is the C_s triplet 4T-3, lying 3.0 kcal/mol (BP86) or 2.7 kcal/mol (M06-L) in energy above the lowest energy structure 4S-1 (Figure 5 and Supporting Information, Table S33). All four carbonyl groups in 4T-3 are discrete four-electron donor η^2 - μ -CO ligands, as suggested by the short Th–O distances of 2.434 Å and 2.434 Å (BP86) or 2.447 Å and 2.451 Å (M06-L). The Th–Th distance of 3.759 Å (BP86) or 3.706 Å (M06-L) is ~ 0.3 Å shorter than that in 4S-1 and 4S-2.

The fourth predicted $\text{Cp}_2\text{Th}_2(\text{CO})_4$ structure is the singlet 4S-4 lying 5.0 kcal/mol (BP86) or 6.9 kcal/mol (M06-L) in energy above the lowest energy structure 4S-1 (Figure 5 and Supporting Information, Table S33). Structure 4S-4 has a central $\text{Th}(\eta^2\text{-}\mu\text{-CO})_3\text{Th}$ unit similar to the lowest energy $\text{Cp}_2\text{Th}_2(\text{CO})_3$ structure 3S-1 with a terminal carbonyl group bonded to the thorium atom attached to only a single oxygen atom. The predicted Th–Th distance of 3.724 Å (BP86) or 3.689 Å (M06-L) is similar to that in 3S-1.

3.4. $\text{Cp}_2\text{Th}_2(\text{CO})_5$ Structures. Seven structures were found for $\text{Cp}_2\text{Th}_2(\text{CO})_5$ (Figure 6 and Supporting Information, Table S34). All of these structures have at least one terminal CO group since five CO groups are at least one too many to bridge a pair of thorium atoms. The lowest energy $\text{Cp}_2\text{Th}_2(\text{CO})_5$

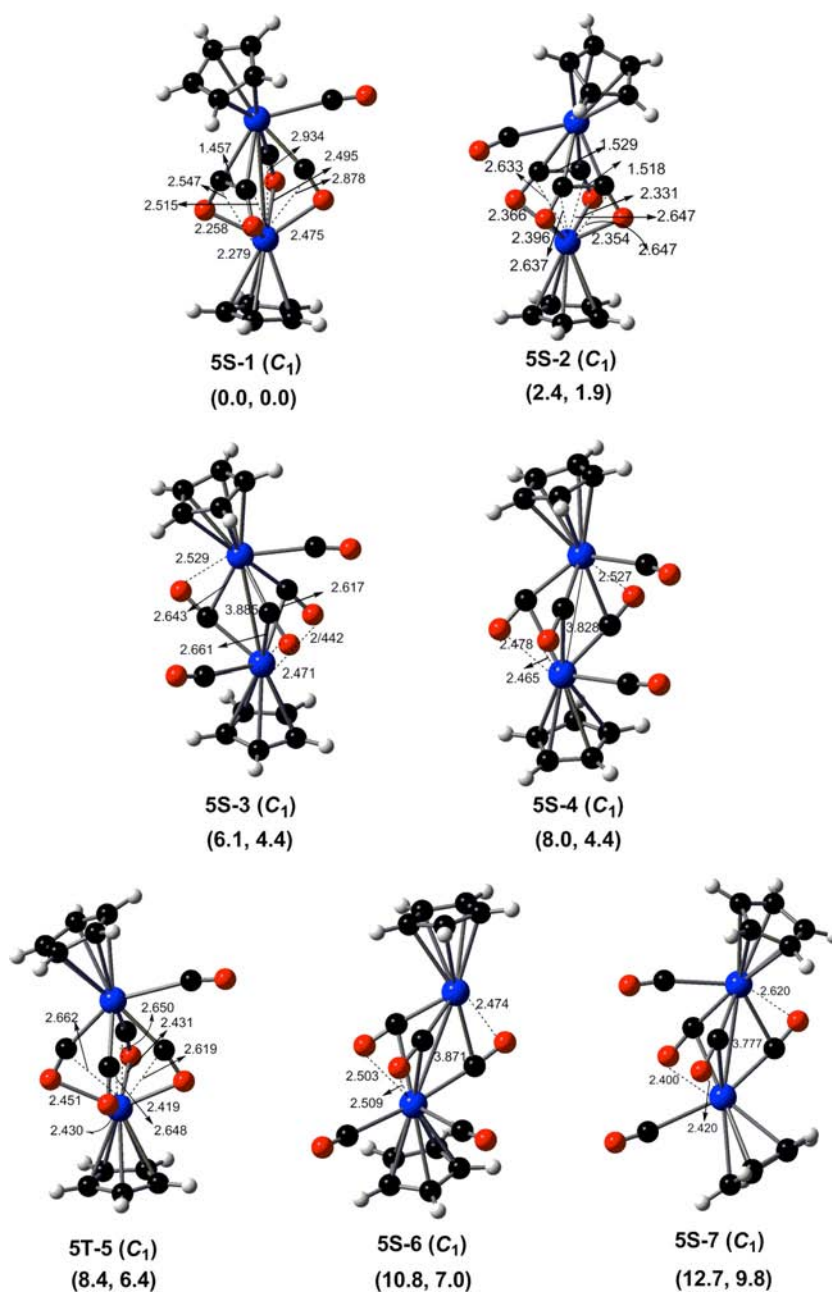


Figure 6. Seven optimized $Cp_2Th_2(CO)_5$ structures.

structure is the C_1 singlet **5S-1**. Structure **5S-1** can be derived from the tetracarbonyl **4S-1** by addition of a terminal carbonyl group to the thorium atom not bonded to the four CO oxygen atoms (the “top” thorium atom in Figure 5). The predicted Th...Th distance in **5S-1** of 4.243 Å (BP86) or 4.191 Å (M06-L) is ~ 0.2 Å longer than that in **4S-1** and clearly indicates the lack of a thorium–thorium bond. The second $Cp_2Th_2(CO)_5$ structure is the C_1 singlet **5S-2**, lying 2.4 kcal/mol (BP86) or 1.9 kcal/mol (M06-L) above **5S-1**. Structure **5S-2** can be derived from the tetracarbonyl structure **4S-2** by adding a terminal carbonyl group to the thorium atom bonded to all four carbonyl carbons. The predicted Th...Th distance of 4.260 Å (BP86) or 4.250 Å (M06-L) in **5S-2** is similar to that in **4S-2**.

The four $Cp_2Th_2(CO)_5$ structures **5S-3**, **5S-4**, **5S-6**, and **5S-7** are all derived from the global minimum $Cp_2Th_2(CO)_3$ structure **3S-1** by adding two terminal carbonyl groups (Figure

6 and Supporting Information, Table S34). The predicted energies above **5S-1** for these four structures are 6.1 kcal/mol (BP86) or 4.4 kcal/mol (M06-L) for **5S-3**, 8.0 kcal/mol (BP86) or 4.4 kcal/mol (M06-L) for **5S-4**, 10.8 kcal/mol (BP86) or 7.0 kcal/mol (M06-L) for **5S-6**, and 12.7 kcal/mol (BP86) or 9.8 kcal/mol (M06-L) for **5S-7**. In **5S-3**, **5S-4**, and **5S-7** each thorium atom bears a single terminal carbonyl group. However, in **5S-6**, the two added terminal carbonyl groups are attached to the same thorium atom. The Th–Th distances of 3.885 Å (BP86) or 3.734 Å (M06-L) in **5S-3**, 3.828 Å (BP86) or 3.790 Å (M06-L) in **5S-4**, 3.871 Å (BP86) or 3.831 Å (M06-L) for **5S-6**, and 3.777 Å (BP86) or 3.714 Å (M06-L) in **5S-7** are 0.1 to 0.2 Å longer than that in **3S-1**.

The only low-lying triplet $Cp_2Th_2(CO)_5$ structure is the C_1 structure **5T-5**, lying 8.4 kcal/mol (BP86) or 6.4 kcal/mol (M06-L) in energy above **5S-1** (Figure 6 and Supporting

Information, Table S34). Structure 5T-5 can be derived from the triplet structure 4T-3 by adding a terminal carbonyl group to the thorium atom bonded only to carbon atoms (the “top” thorium atom in Figure 5). The predicted Th–Th distance in 5T-5 of 3.806 Å (BP86) or 3.727 Å (M06-L) is similar to that in 4T-3.

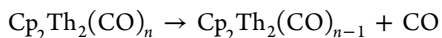
3.5. Dissociation and Disproportionation Reactions.

Table 1 reports the energies of the following single carbonyl

Table 1. Dissociation Energies and Disproportionation Energies (kcal/mol) Based on the Lowest Energy $\text{Cp}_2\text{Th}_2(\text{CO})_n$ Structures ($n = 3$ to 5)

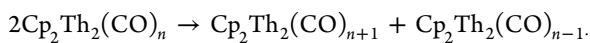
	BP86	M06-L
$\text{Cp}_2\text{Th}_2(\text{CO})_5$ (5S-1) \rightarrow $\text{Cp}_2\text{Th}_2(\text{CO})_4$ (4S-1) + CO	13.6	14.6
$\text{Cp}_2\text{Th}_2(\text{CO})_4$ (4S-1) \rightarrow $\text{Cp}_2\text{Th}_2(\text{CO})_3$ (3S-1) + CO	21.7	23.6
$\text{Cp}_2\text{Th}_2(\text{CO})_3$ (3S-1) \rightarrow $\text{Cp}_2\text{Th}_2(\text{CO})_2$ (2S-1) + CO	43.7	41.3
2 $\text{Cp}_2\text{Th}_2(\text{CO})_4$ (4S-1) \rightarrow $\text{Cp}_2\text{Th}_2(\text{CO})_5$ (5S-1) + $\text{Cp}_2\text{Th}_2(\text{CO})_3$ (3S-1)	8.1	9.0
2 $\text{Cp}_2\text{Th}_2(\text{CO})_3$ (3S-1) \rightarrow $\text{Cp}_2\text{Th}_2(\text{CO})_4$ (4S-1) + $\text{Cp}_2\text{Th}_2(\text{CO})_2$ (2S-1)	22.0	17.7

dissociation reactions for the energy $\text{Cp}_2\text{Th}_2(\text{CO})_n$ structures ($n = 5$ to 3), based on the lowest energy structures.



The CO bond dissociation energy of 14.6 kcal/mol (M06-L) for a single carbonyl loss from $\text{Cp}_2\text{Th}_2(\text{CO})_5$ to give $\text{Cp}_2\text{Th}_2(\text{CO})_4$ is significantly lower than the experimental values of 27 kcal/mol, 41 kcal/mol, and 37 kcal/mol for the simple carbonyls $\text{Ni}(\text{CO})_4$, $\text{Fe}(\text{CO})_5$, and $\text{Cr}(\text{CO})_6$, respectively, of the d-block metals.⁵¹ This suggests that terminal CO groups are significantly more weakly bonded to f-block transition metals such as thorium than to the usual d-block metals. This is consistent with the experimentally observed facile loss of the coordinated CO ligand in Cp_3UCO derivatives.^{9,10} However, the CO dissociation energies are significantly larger for the $\text{Cp}_2\text{Th}_2(\text{CO})_n$ ($n = 4, 3$) derivatives which no longer have terminal CO groups. Thus the CO dissociation energy of $\text{Cp}_2\text{Th}_2(\text{CO})_4$ to give $\text{Cp}_2\text{Th}_2(\text{CO})_3$ is predicted to be ~ 23 kcal/mol. The predicted energy required to break up the central $\text{Th}(\eta^2\text{-}\mu\text{-CO})_3\text{Th}$ unit in the $\text{Cp}_2\text{Th}_2(\text{CO})_3$ structure 3S-1 is even greater as indicated by its large CO dissociation energy of ~ 43 kcal/mol to give the $\text{Cp}_2\text{Th}_2(\text{CO})_2$ structure 2S-1.

Table 1 also shows the energies for the following disproportionation reactions:



In this connection the disproportionation of $\text{Cp}_2\text{Th}_2(\text{CO})_3$ into $\text{Cp}_2\text{Th}_2(\text{CO})_4$ + $\text{Cp}_2\text{Th}_2(\text{CO})_2$ is seen to be significantly endothermic at ~ 20 kcal/mol, suggesting that $\text{Cp}_2\text{Th}_2(\text{CO})_3$ is a viable species. In addition the analogous disproportionation of $\text{Cp}_2\text{Th}_2(\text{CO})_4$ into $\text{Cp}_2\text{Th}_2(\text{CO})_5$ + $\text{Cp}_2\text{Th}_2(\text{CO})_3$ is also endothermic at ~ 9 kcal/mol suggesting the possible viability of $\text{Cp}_2\text{Th}_2(\text{CO})_4$.

The dissociation of the binuclear derivatives $\text{Cp}_2\text{Th}_2(\text{CO})_n$ into mononuclear $\text{CpTh}(\text{CO})_m$ derivatives was also investigated (Table 2). To obtain such data the geometries of all of the mononuclear $\text{CpTh}(\text{CO})_m$ derivatives ($m = 5, 4, 3, 2, 1$) were optimized using the same theoretical methods as for the binuclear derivatives (Figure 7 and Supporting Information). In

Table 2. Energies (kcal/mol) for the Dissociation of $\text{Cp}_2\text{Th}_2(\text{CO})_n$ ($n = 5$ to 3) into Mononuclear Fragments $\text{CpTh}(\text{CO})_m$ ($m = 1$ to 5)

	BP86	M06-L
$\text{Cp}_2\text{Th}_2(\text{CO})_5$ (5S-1) \rightarrow $\text{CpTh}(\text{CO})_3$ + $\text{CpTh}(\text{CO})_2$	99.5	111.6
$\text{Cp}_2\text{Th}_2(\text{CO})_5$ (5S-1) \rightarrow $\text{CpTh}(\text{CO})_4$ + $\text{CpTh}(\text{CO})$	103.1	116.3
$\text{Cp}_2\text{Th}_2(\text{CO})_4$ (4S-1) \rightarrow 2 $\text{CpTh}(\text{CO})_2$	115.6	128.4
$\text{Cp}_2\text{Th}_2(\text{CO})_4$ (4S-1) \rightarrow $\text{CpTh}(\text{CO})_3$ + $\text{CpTh}(\text{CO})$	119.5	132.6
$\text{Cp}_2\text{Th}_2(\text{CO})_3$ (3S-1) \rightarrow $\text{CpTh}(\text{CO})_2$ + $\text{CpTh}(\text{CO})$	128.6	139.9

this connection the dissociation energies for all the $\text{Cp}_2\text{Th}_2(\text{CO})_n$ structures into mononuclear $\text{CpTh}(\text{CO})_m$ derivatives are predicted to be very large, in excess of 99 kcal/mol. The high energies for the dissociation of $\text{Cp}_2\text{Th}_2(\text{CO})_n$ into mononuclear $\text{CpTh}(\text{CO})_m$ fragments appear to relate to the stability of the central $\text{Th}(\eta^2\text{-}\mu\text{-CO})_3\text{Th}$ and $\text{Th}(\eta^4\text{-}\mu\text{-C}_2\text{O}_2)(\eta^2\text{-}\mu\text{-CO})_2$ units in the $\text{Cp}_2\text{Th}_2(\text{CO})_n$ derivatives. Furthermore, the dissociation energies for $\text{Cp}_2\text{Th}_2(\text{CO})_n$ into mononuclear fragments increase monotonically with decreasing numbers of carbonyl groups. Such dissociation energies change only slightly when comparing the symmetrical dissociation and the unsymmetrical dissociation. We therefore conclude that the mononuclear $\text{CpTh}(\text{CO})_m$ fragments are not likely to play an important role in the chemistry of the binuclear $\text{Cp}_2\text{Th}_2(\text{CO})_n$ derivatives.

3.6. Natural Bond Orbital Analysis of the $\text{Cp}_2\text{Th}_2(\text{CO})_n$ Derivatives. To obtain more insight into the chemical bonding in the $\text{Cp}_2\text{Th}_2(\text{CO})_n$ derivatives, the Th–Th natural charges and the Wiberg bond indices (WBIs) for the Th–Th interactions were determined from Weinhold Natural Bond Orbital (NBO) analyses⁵² using the BP86 method (Table 3). For the $\text{Cp}_2\text{Th}_2(\text{CO})_3$ and $\text{Cp}_2\text{Th}_2(\text{CO})_4$ structures without terminal CO groups, the natural charges on the thorium atoms are positive, in the range +1.1 to +1.5. Within this range the thorium atoms bonded to the oxygen atoms of the bridging CO groups have more positive natural charges than the thorium atoms bonded only to the carbon atoms of the bridging CO groups. Addition of terminal CO groups to a thorium atom in the carbonyl-rich $\text{Cp}_2\text{Th}_2(\text{CO})_5$ structures increases the negative charge on the thorium atom bearing the terminal CO groups and increases the positive charge on the thorium atom without terminal carbonyls.

The Wiberg Bond Indices (WBIs) of the $\text{Cp}_2\text{Th}_2(\text{CO})_n$ derivatives are also listed in Table 3. Because of the lack of experimental examples of compounds having Th–Th bonds of any type, there is little guidance as to what WBIs to expect for a given formal metal–metal bond order involving f-block metals. The WBIs found for the $\text{Cp}_2\text{Th}_2(\text{CO})_n$ derivatives fall into three broad categories. Those for the structures having central $\text{Th}(\eta^2\text{-}\mu\text{-CO})_3\text{Th}$ units with three bridging CO groups and Th–Th distances ranging from 3.7 to 3.9 Å have WBIs ranging from 0.42 to 0.52. The WBIs found for the structures having central $\text{Th}(\eta^2\text{-}\mu\text{-CO})_2(\eta^4\text{-}\mu\text{-C}_2\text{O}_2)\text{Th}$ units with four bridging CO groups (two as a C_2O_2 ligand) and Th–Th distances ranging from 4.0 to 4.4 Å range from 0.17 to 0.27. The two $\text{Cp}_2\text{Th}_2(\text{CO})_2$ structures 2S-1 and 2S-2 with significantly shorter Th–Th distances ranging from 3.3 to 3.4 Å have much higher WBIs ranging from 0.81 to 0.87. These predicted Th–Th distances of 3.3 to 3.4 Å for the $\text{Cp}_2\text{Th}_2(\text{CO})_2$ structures 2S-1 and 2S-2 are close to the standard Th–Th single bond distance of 3.50 Å estimated from the calculated Th double bond covalent radius.⁵³ We suspect that these may be the only

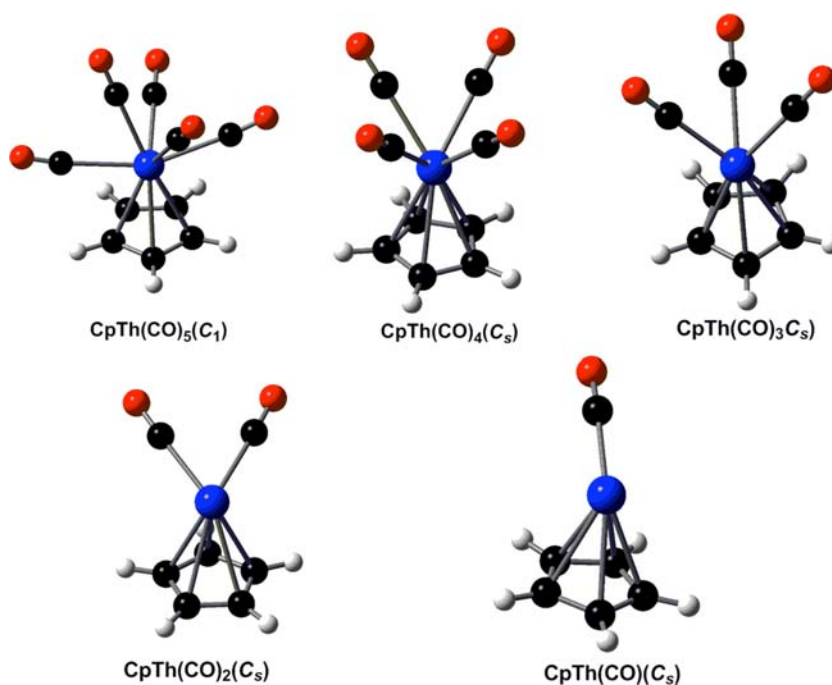


Figure 7. Optimized structures of the mononuclear fragments $\text{CpTh}(\text{CO})_n$ ($n = 5, 4, 3, 2, 1$).

Table 3. Atomic Charges and Wiberg Bond Indices, Compared with the Th–Th Bond Distances (in Å) for the $\text{Cp}_2\text{Th}_2(\text{CO})_n$ Singlet Structures by the BP86 Method

	natural charges on Th1/Th2	Wiberg bond index	Th–Th distance (Å)	number of $\eta^2\text{-}\mu\text{-CO}$ groups
$(\text{C}_5\text{H}_5)_2\text{Th}_2(\text{CO})_5$ (5S-1)	+0.66/+1.60	0.21	4.243	4
$(\text{C}_5\text{H}_5)_2\text{Th}_2(\text{CO})_5$ (5S-2)	+0.99/+1.61	0.17	4.360	4
$(\text{C}_5\text{H}_5)_2\text{Th}_2(\text{CO})_5$ (5S-3)	+0.72/+0.73	0.42	3.885	3
$(\text{C}_5\text{H}_5)_2\text{Th}_2(\text{CO})_5$ (5S-4)	+0.58/+0.68	0.47	3.828	3
$(\text{C}_5\text{H}_5)_2\text{Th}_2(\text{CO})_5$ (5T-5)	+0.26/+1.18	0.43	3.806	4
$(\text{C}_5\text{H}_5)_2\text{Th}_2(\text{CO})_5$ (5S-6)	+1.17/+0.00	0.46	3.871	3
$(\text{C}_5\text{H}_5)_2\text{Th}_2(\text{CO})_5$ (5S-7)	+0.66/+0.75	0.52	3.777	3
$(\text{C}_5\text{H}_5)_2\text{Th}_2(\text{CO})_4$ (4S-1)	+1.14/+1.46	0.27	4.062	4
$(\text{C}_5\text{H}_5)_2\text{Th}_2(\text{CO})_4$ (4S-2)	+1.33/+1.47	0.25	4.030	4
$(\text{C}_5\text{H}_5)_2\text{Th}_2(\text{CO})_4$ (4T-3)	+0.83/+1.15	0.44	3.759	4
$(\text{C}_5\text{H}_5)_2\text{Th}_2(\text{CO})_4$ (4S-4)	+0.65/+1.33	0.51	3.724	3
$(\text{C}_5\text{H}_5)_2\text{Th}_2(\text{CO})_3$ (3S-1)	+1.12/+1.29	0.49	3.699	3
$(\text{C}_5\text{H}_5)_2\text{Th}_2(\text{CO})_3$ (3S-2)	+1.11/+1.50	0.42	3.922	3
$(\text{C}_5\text{H}_5)_2\text{Th}_2(\text{CO})_2$ (2S-1)	+1.10/+1.14	0.81	3.337	2
$(\text{C}_5\text{H}_5)_2\text{Th}_2(\text{CO})_2$ (2S-2)	+1.28/+1.28	0.87	3.408	2

$\text{Cp}_2\text{Th}_2(\text{CO})_n$ derivatives reported in this paper with a direct Th–Th bond. However, an AIM analysis^{54,55} of the two lowest energy $\text{Cp}_2\text{Th}_2(\text{CO})_2$ structures 2S-1 and 2S-2 using multiwfn software⁵⁶ indicates the lack of a bond critical point between

the thorium atoms (Figure 8). This suggests that there is no actual two-center two-electron Th–Th bond in each

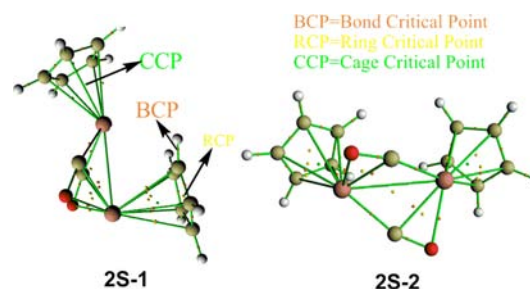


Figure 8. QTAIM analysis of the two $\text{Cp}_2\text{Th}_2(\text{CO})_2$ structures.

$\text{Cp}_2\text{Th}_2(\text{CO})_2$ structure. Instead the formal Th–Th “single bond” in $\text{Cp}_2\text{Th}_2(\text{CO})_2$ is actually a multicenter bond involving the bridging CO groups. This is confirmed by both Kohn–Sham and natural bond orbitals (NBOs) of the two $\text{Cp}_2\text{Th}_2(\text{CO})_2$ structures (Figure 9). The situation in $\text{Cp}_2\text{Th}_2(\text{CO})_2$ thus may be similar to that in the triply bridged $\text{Fe}_2(\text{CO})_9$ structure where the Fe–Fe distance and electron counting suggest a formal single bond but AIM and related methods of analysis suggest the absence of a direct iron–iron bond.^{57,58}

Note that if the carbonyl ligands in the $\text{Cp}_2\text{Th}_2(\text{CO})_2$ structures are CO^{2-} dianions, then the formal oxidation state of each thorium atom is only +3 rather than the favored +4. A formal Th–Th bond is much more likely between thorium atoms in the +3 formal oxidation state than in the common +4 oxidation state. This interpretation suggests the WBIs in the $\text{Cp}_2\text{Th}_2(\text{CO})_n$ derivatives to approach the actual formal bond orders. If this is the case, then the actinides differ significantly from the d-block metals for which the WBI values are typically only 20 to 30% of the actual formal metal–metal bond orders.⁵⁹ However, neither Kohn–Sham and natural bond orbitals (NBOs) support a pure localized Th–Th single bond

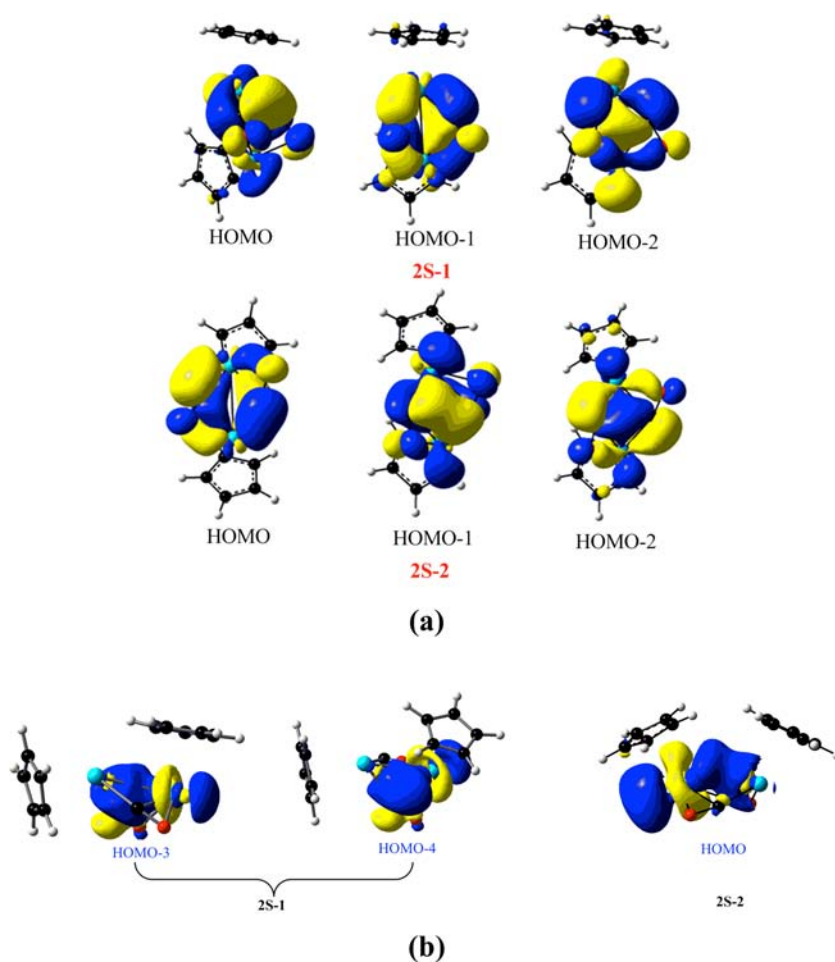


Figure 9. (a) Kohn–Sham and (b) natural bond orbitals (NBOs) of the two $\text{Cp}_2\text{Th}_2(\text{CO})_2$ structures mainly representing the Th–Th interaction (isovalue = 0.03).

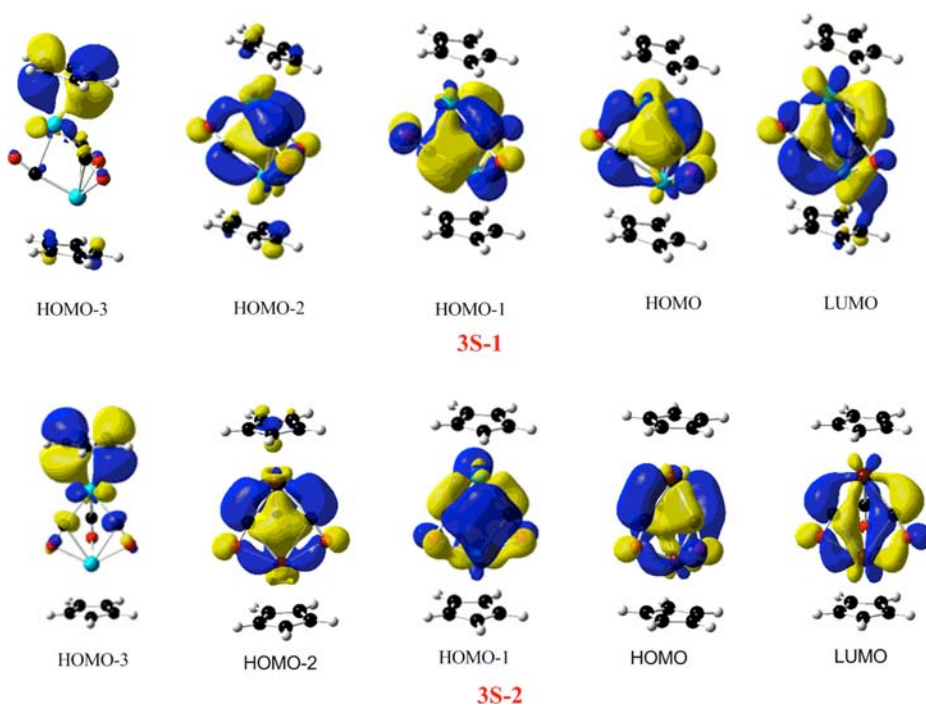


Figure 10. Frontier MOs of the $\text{Cp}_2\text{Th}_2(\eta^2\text{-}\mu\text{-CO})_3$ structures 3S-1 and 3S-2 (isovalue of 0.03).

in these $\text{Cp}_2\text{Th}_2(\text{CO})_2$ structures. Instead the interaction between the thorium atoms involves multicenter bonding including orbitals from the bridging CO groups.

3.7. Molecular Orbital Analysis. To gain more insight into the bonding in the central $\text{Th}(\mu\text{-CO})_n\text{Th}$ ($n = 3, 4$) units in the $\text{Cp}_2\text{Th}_2(\text{CO})_n$ structures discussed in this paper, their frontier molecular orbitals (MOs) were examined (Figures 9, 10, and 11). For the $\text{Cp}_2\text{Th}_2(\text{CO})_3$ structures **3S-1** and **3S-2**,

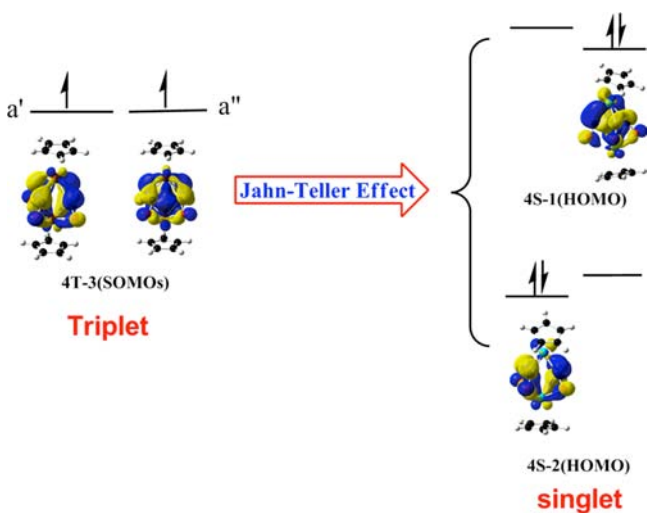


Figure 11. Highest-lying filled MOs (SOMOs and HOMOs) of the $\text{Cp}_2\text{Th}_2(\text{CO})_4$ structures **4S-1**, **4S-2**, and **4S-3**.

the three highest bonding MOs (highest occupied MO (HOMO) down to HOMO–2 in Figure 10) involve interactions between the two thorium atoms and the three bridging CO groups, without the Cp rings playing a significant role. These frontier bonding MOs thus appear to correspond to the strong $\text{Th}\rightarrow\text{CO}$ back-bonding present in these systems as, for example, reflected by their very low $\nu(\text{CO})$ frequencies. The bonding MOs immediately below HOMO–2 (e.g., HOMO–3 and lower) appear to involve mainly interactions between the thorium atoms and the Cp rings.

The frontier molecular orbitals for the $\text{Cp}_2\text{Th}_2(\text{CO})_4$ structures **4S-1**, **4S-2**, and **4T-3** suggest a novel type of Jahn–Teller distortion involving these three structures (Figure 11). The central $\text{Th}(\eta^2\text{-}\mu\text{-CO})_4\text{Th}$ unit in the triplet structure **4T-3** has 4-fold symmetry with equivalent nonbonding distances between the carbon atoms of the bridging CO groups. The two singly occupied MOs (SOMOs) in **4T-3** (a' and a'') are very similar to the b_{1g} and a_{2u} MOs in the recently reported triplet ground state of the neutral oxocarbon C_4O_4 .⁶⁰ In ideal C_4 symmetry of the central $\text{Th}(\eta^2\text{-}\mu\text{-CO})_4\text{Th}$ unit of **4T-3** these two orbitals would be degenerate. The symmetry breaking in **4T-3** from the Cp rings is small enough to make the energy separation between these SOMOs less than the electron pairing energy, so that they remain effectively degenerate. Pairing of these electrons in the singlet structures **4S-1** and **4S-2** leads to splitting of these nearly degenerate orbitals and the symmetry breaking associated with the Jahn–Teller effect. This symmetry breaking brings the carbon atoms of two of the CO groups close enough together to form a C–C bond, leading to the bridging $\eta^4\text{-}\mu\text{-C}_2\text{O}_2$ ligand in structures **4S-1** and **4S-2**.

3.8. Carbonyl Vibrational Frequencies. The infrared $\nu(\text{CO})$ frequencies of metal carbonyl derivatives correlate with the effective C–O bond orders and thus can assess the relative

contribution of canonical structures I, II, and III (Figure 2) in the interaction of a CO group with a metal atom. The $\nu(\text{CO})$ frequencies are thus a good way to estimate the amount of back bonding in a metal carbonyl derivative. In this connection the CO groups in the $\text{Cp}_2\text{Th}_2(\text{CO})_n$ derivatives (Table 4) fall into

Table 4. Harmonic $\nu(\text{CO})$ Vibrational Frequencies (in cm^{-1}) and Infrared Intensities (in Parentheses, in km/mol) for the $\text{Cp}_2\text{Th}_2(\text{CO})_n$ Derivatives

2S-1	1223(419), 1301(220)
2S-2	1245(520), 1315(85)
3S-1	1350(460), 1396(740), 1513(70)
3S-2	1281(249), 1327(561), 1401(35)
4S-1	1211(43), 1241(256), 1471(374), 1547(276)
4S-2	1275(348), 1316(110), 1359(224), 1392(161)
4T-3	1442(6), 1444(628), 1444(622), 1550(83)
5S-1	1167(52), 1231(331), 1469(303), 1544(503), 1981(1112)
5S-2	1227(227), 1285(92), 1316(172), 1365(240), 1993(596)

two categories: (1) The $\nu(\text{CO})$ frequencies of the bridging CO groups in the central $\text{Th}(\eta^2\text{-}\mu\text{-CO})_3\text{Th}$ and $\text{Th}(\eta^4\text{-C}_2\text{O}_2)(\eta^2\text{-}\mu\text{-CO})_2\text{Th}$ units; (2) The $\nu(\text{CO})$ frequencies of the terminal CO groups in the carbonyl-rich $\text{Cp}_2\text{Th}_2(\text{CO})_5$ structures.

The $\nu(\text{CO})$ frequency of the single terminal CO group in the lowest energy $\text{Cp}_2\text{Th}_2(\text{CO})_5$ structure **5S-1** (Figure 5) of 1988 cm^{-1} is similar to the terminal $\nu(\text{CO})$ frequencies of cyclopentadienylmetal carbonyls of the d-block transition metals. For such terminal CO groups the metal–CO bonding can be represented as a resonance hybrid of valence structure I with a formal $\text{C}\equiv\text{O}$ triple and II with a formal $\text{C}=\text{O}$ double bond (Figure 2).

The situation is very different for the $\nu(\text{CO})$ frequencies for the bridging carbonyls in the central $\text{Th}(\eta^2\text{-}\mu\text{-CO})_3\text{Th}$ and $\text{Th}(\eta^4\text{-C}_2\text{O}_2)(\eta^2\text{-}\mu\text{-CO})_2\text{Th}$ units in the $\text{Cp}_2\text{Th}_2(\text{CO})_n$ structures. For such bridging CO groups (and bridging C_2O_2 groups) the $\nu(\text{CO})$ frequencies range from 1281 to 1513 cm^{-1} in structures with central $\text{Th}(\eta^2\text{-}\mu\text{-CO})_3\text{Th}$ units and even lower from 1167 to 1547 cm^{-1} in structures with central $\text{Th}(\eta^4\text{-C}_2\text{O}_2)(\eta^2\text{-}\mu\text{-CO})_2\text{Th}$ units. No compounds are known experimentally for the d-block transition metals with comparable $\text{M}(\eta^2\text{-}\mu\text{-CO})_3\text{M}$ and $\text{M}(\eta^4\text{-C}_2\text{O}_2)(\eta^2\text{-}\mu\text{-CO})_2\text{M}$ units. However, the $\nu(\text{CO})$ frequencies for a titanium structure $\text{CpTi}(\eta^2\text{-}\mu\text{-CO})_3\text{TiCp}$ analogous to **3S-1** are predicted to be 1501, 1540, and 1603 cm^{-1} using the same BP86 functional.²⁹ Thus the predicted $\nu(\text{CO})$ frequencies for **3S-1** are 90 to 150 cm^{-1} lower than those in the analogous titanium compound, indicating extreme back bonding from the thorium atom to these bridging CO groups in **3S-1**. This suggests that a major contribution to the thorium–CO bond in **3S-1** is the canonical structure III with a formal C–O single bond (Figure 2). Thus the bridging CO groups in **3S-1** and other structures with the same central $\text{Th}(\eta^2\text{-}\mu\text{-CO})_3\text{Th}$ unit may be regarded formally as dianions derived from the double deprotonation of the hydroxycarbene ligand: $\text{C}(\text{H})(\text{OH})$, which has a C–O single bond. The back-donation of electrons from the thorium atoms to the bridging CO groups in the central $\text{Th}(\eta^2\text{-}\mu\text{-CO})_3\text{Th}$ unit is so extreme that all three CO groups are effectively reduced to CO^{2-} dianions. Since the Cp rings are monoanions, the formal oxidation states of the thorium atoms in $\text{Cp}_2\text{Th}_2(\eta^2\text{-}\mu\text{-CO})_3$ and its carbonylation products is the highly favored thorium +4 oxidation state. In $\text{Cp}_2\text{Th}_2(\eta^4\text{-}\mu\text{-C}_2\text{O}_2)(\eta^2\text{-}\mu\text{-CO})_2$ and its carbonylation products the thorium atoms are also in the

favored +4 oxidation state, since the bridging C_2O_2 ligand appears to be the ethynediolate dianion. However, in the $Cp_2Th_2(CO)_2$ structures **2S-1** and **2S-2** (Figure 3 and Supporting Information, Table S35) the thorium atoms are only in the +3 formal oxidation state. Although the ~ 3.3 to ~ 3.4 Å Th–Th distances and ~ 0.8 WBIs (Table 3) in the $Cp_2Th_2(CO)_2$ structures might suggest a formal single bond, the interactions between the two thorium atoms appear to occur through multicenter bonding involving the bridging CO ligands. The Th–Th interactions in these $Cp_2Th_2(CO)_2$ structures thus appears somewhat analogous to the Fe–Fe interaction in the well-known $Fe_2(CO)_9$.^{58,59}

4. DISCUSSION

The most favorable $Cp_2Th_2(CO)_n$ structures in terms of the thermochemistry appear to be $Cp_2Th_2(\eta^2-\mu-CO)_3$ (**3S-1**) and $Cp_2Th_2(\eta^4-C_2O_2)(\eta^2-\mu-CO)$ (**4S-1**). These structures are very different than any of the structures of known binuclear cyclopentadienylmetal carbonyls of the d-block transition metals. However, a theoretical study on the titanium derivatives $Cp_2Ti_2(CO)_n$ predicts an analogous $Cp_2Ti_2(\eta^2-\mu-CO)_3$ structure to be one of the most favorable structures.²⁹ The back bonding of the central thorium atoms to the bridging CO groups in the $Cp_2Th_2(CO)_n$ structures appears to be very strong. This leads to $\nu(CO)$ frequencies lower than those found or predicted theoretically for the d-block transition metals and in a reasonable range for C–O single bonds. In fact, the thorium back bonding to these bridging CO ligands is so strong that these ligands can be regarded formally as CO^{2-} dianions, derived from the deprotonation of hydroxycarbene, $:C(H)-(OH)$. For $Cp_2Th_2(\eta^2-\mu-CO)_3$ (**3S-1**) this leads to the favorable formal oxidation state of +4 for the central thorium atoms.

Another feature of the relatively favorable $Cp_2Th_2(\eta^4-\mu-C_2O_2)(\eta^2-\mu-CO)_2$ structure **4S-1** is the coupling of two CO ligands to form a bridging C_2O_2 ligand. Such coupling of CO ligands is not known in the carbonyl chemistry of the d-block transition metals. However, related couplings of CF ligands to form C_2F_2 ligands,^{61,62} BF ligands to form B_2F_2 ligands,⁶³ and BO ligands to form B_2O_2 ligands⁶⁴ in derivatives of the d-block metals are all predicted from recent theoretical studies. The C_2O_2 ligand in the $Cp_2Th_2(\eta^4-\mu-C_2O_2)(\eta^2-\mu-CO)_2$ structure **4S-1** may be regarded as the dianion of ethynediol, $HOC\equiv COH$. Coordination of the $C\equiv C$ triple bond of $HOC\equiv COH$ to one of the thorium atoms combined with strong $Th\rightarrow C_2O_2$ back bonding reduces the effective carbon–carbon bond order in the ethynediolate ligand to approximately one, as indicated by the predicted C–C single bond distance of ~ 1.48 Å. The reduction and coupling of two CO ligands to a coordinated $C_2O_2^{2-}$ ligand is again a manifestation of the extremely strong back bonding of actinides to CO groups. Such a process appears to be related to the experimentally observed reductive coupling of CO with organoactinide complexes to give ethynediolate, deltate, and squarate complexes.^{20,21} The thorium atoms in $Cp_2Th_2(\eta^4-\mu-C_2O_2)(\eta^2-\mu-CO)_2$ are in the favored +4 formal oxidation state if the separate CO groups are considered as hydroxycarbene dianions and the coupled C_2O_2 ligand is considered as the ethynediolate dianion.

Stable actinide derivatives containing metal–metal bonds between two actinide atoms are essentially unknown although such bonding in the simple dimers An_2 ($An = Ac, Th, Pa,$ and U) has been the subject of theoretical studies.^{65,66} The favorable +4 thorium formal oxidation states in the

$Cp_2Th_2(CO)_n$ derivatives arising from the extreme back bonding of the thorium to the bridging ligands to give the CO^{2-} and $C_2O_2^{2-}$ dianions make a true direct thorium–thorium bond unlikely in these species. The Wiberg Bond Indices (WBIs) for the Th–Th interactions in the $Cp_2Th_2(CO)_n$ ($n = 3$ to 5) derivatives are significantly less than unity. Their relatively small values can thus reflect indirect weaker Th–Th interactions through the $(CO)_n$ bridging system rather than direct Th–Th bonds. Thus the WBIs for the structures having central $Th(\eta^2-\mu-CO)_3Th$ units and Th–Th distances from 3.7 to 3.9 Å range from 0.42 to 0.51. The WBIs for the structures having central $Th(\eta^2-\mu-CO)_2(\eta^4-\mu-C_2O_2)Th$ units and Th–Th distances ranging from 4.0 to 4.6 Å have WBIs in the range 0.17 to 0.27. However, the dicarbonyl structures **2S-1** and **2S-2** with significantly shorter Th–Th distances of 3.3 to 3.4 Å have WBIs of ~ 0.8 much closer to unity. Neither the AIM analysis nor the frontier molecular orbital analysis supports a formal two-center two-electron Th–Th single bond in these $Cp_2Th_2(CO)_2$ structures. Instead, the Th–Th interactions in these structures appear to involve multicenter bonding including orbitals from the bridging carbonyl ligands. In the two dicarbonyl structures **2S-1** and **2S-2** the thorium atoms exhibit the +3 formal oxidation state rather than the favorable +4 oxidation state suggested for the carbonyl richer $Cp_2Th_2(CO)_n$ ($n = 3, 4, 5$) structures.

Most of the triplet $Cp_2Th_2(CO)_n$ structures were found to have energies too high to be of chemical significance and therefore are not discussed in this paper. The exceptions are the $Cp_2Th_2(CO)_4$ structure **4T-3** and its carbonylation product **5T-5**. Structure **4T-3**, lying within 3 kcal/mol of the lowest energy $Cp_2Th_2(CO)_4$ structure **4S-1**, has four $\eta^2-\mu-CO$ groups, which, unlike those in the isomeric singlet structure **4S-1**, are not coupled. The spin density in **4T-3** is largely delocalized in the four CO bridges (Figure 12). If two of the bridging CO

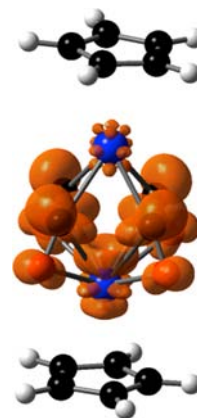


Figure 12. Spin density in the triplet $Cp_2Th_2(CO)_4$ structure **4T-3**.

groups in **4T-3** are CO^{2-} dianions and the other two are $CO^{\bullet-}$ radical anions, then the thorium atoms have the favored +4 oxidation state. The unpaired electrons in the $CO^{\bullet-}$ radical anions can then be delocalized among all four CO groups in accord with the spin density.

5. SUMMARY

The most favorable $Cp_2Th_2(CO)_n$ structures in terms of energy and thermochemistry are the tricarbonyl $Cp_2Th_2(\eta^2-\mu-CO)_3$ (**3S-1**) having three four-electron donor bridging $\eta^2-\mu-CO$ groups and the tetracarbonyl $Cp_2Th_2(\eta^4-\mu-C_2O_2)(\eta^2-\mu-CO)_2$

(4S-1) having two four-electron donor bridging $\eta^2\text{-}\mu\text{-CO}$ groups and a bridging $\eta^4\text{-}\mu\text{-C}_2\text{O}_2$ group. Considering the bridging CO and C_2O_2 groups in these structures as dianions derived from the double deprotonations of hydroxycarbene (:C(H)(OH)) and ethynediol (HOC \equiv COH), respectively, leads to the favorable +4 formal oxidation state for the thorium atoms. The reduction of CO to the dianionic CO^{2-} and $\text{C}_2\text{O}_2^{2-}$ ligands in these systems appears to be the result of extreme Th \rightarrow CO back bonding as indicated by extremely low $\nu(\text{CO})$ frequencies of 1167 to 1550 cm^{-1} of the central Th($\eta^2\text{-}\mu\text{-CO}$) $_3$ Th and Th($\eta^4\text{-}\mu\text{-C}_2\text{O}_2$)($\eta^2\text{-}\mu\text{-CO}$) $_2$ Th units of these structures. Furthermore, the reductive coupling of two CO ligands to form the ethynediolate ligand in $\text{Cp}_2\text{Th}_2(\eta^4\text{-}\mu\text{-C}_2\text{O}_2)(\eta^2\text{-}\mu\text{-CO})_2$ appears to be related to the experimentally observed^{20,21} coupling of CO ligands by actinides, particularly uranium(III) complexes, to give not only ethynediolate complexes but also deltate ($\text{C}_3\text{O}_3^{2-}$) and squarate ($\text{C}_4\text{O}_4^{2-}$) uranium(IV) complexes.

A characteristic of the $\text{Cp}_2\text{Th}_2(\eta^2\text{-}\mu\text{-CO})_3$ and $\text{Cp}_2\text{Th}_2(\eta^4\text{-}\mu\text{-C}_2\text{O}_2)(\eta^2\text{-}\mu\text{-CO})_2$ structures is the ability to add terminal CO groups, preferably to the thorium atom bonded to the fewest oxygen atoms. These terminal CO groups exhibit terminal $\nu(\text{CO})$ frequencies in the typical range for terminal CO groups in d-block metal carbonyls. However, these terminal CO groups are only weakly bonded to the thorium atoms as indicated by a predicted CO dissociation energy of ~ 14 kcal/mol for $\text{Cp}_2\text{Th}_2(\text{CO})_5$.

■ ASSOCIATED CONTENT

■ Supporting Information

Tables S1 to S15: Optimized coordinates of the reported $\text{Cp}_2\text{Th}_2(\text{CO})_n$ ($n = 2$ to 5) structures; Tables S16 to S30: Harmonic vibrational frequencies and infrared intensities (in the $\text{Cp}_2\text{Th}_2(\text{CO})_n$ ($n = 2$ to 5) structures; Table S31: Total energies (E , in Hartree) of the global minima of $\text{CpTh}(\text{CO})_n$ ($n = 5, 4, 3, 2, 1$); Figure S1: Optimized structures of the mononuclear fragments $\text{CpTh}(\text{CO})_n$ ($n = 5, 4, 3, 2, 1$); Table S32 to S35: Total energies (E in hartree), relative energies (ΔE in kcal/mol), Th–Th Distances (\AA), numbers of imaginary vibrational frequencies (Nimg), and spin expectation values $\langle S^2 \rangle$ for the $\text{Cp}_2\text{Th}_2(\text{CO})_n$ ($n = 2$ to 5) structures; Complete Gaussian09 reference (Reference 49). This material is available free of charge via the Internet at <http://pubs.acs.org>.

■ AUTHOR INFORMATION

Corresponding Author

*E-mail: rbking@chem.uga.edu (R.B.K.), fenghao@mail.xhu.edu.cn (H.F.).

Notes

The authors declare no competing financial interest.

■ ACKNOWLEDGMENTS

This research was supported by the Program for New Century Excellent Talents in University in China (Grant NCET-10-0949), the Chinese National Natural Science Foundation (Grants 11174236 and 11074204), and the U.S. National Science Foundation (Grants CHE-1057466 and CHE-1054286). H.L. thanks the Center for Computational Quantum Chemistry at the University of Georgia for hospitality during his six-month visit in 2012.

■ REFERENCES

- (1) Schützenberger, P. *Bull. Soc. Chim. Fr.* **1868**, *10*, 188.
- (2) Mond, L.; Langer, C.; Quincke, F. *J. Chem. Soc.* **1890**, *57*, 749.
- (3) Calderazzo, F. In *Encyclopedia of Inorganic Chemistry*, 2nd ed.; King, R. B., Ed.; Wiley: Chichester, U.K., 2005; pp 764–781.
- (4) Elschenbroich, C. *Organometallics*; Wiley-VCH: Weinheim, Germany, 2006; Chapter 14.4.
- (5) Szilagy, R. K.; Frenking, G. *Organometallics* **1997**, *16*, 4807.
- (6) Diefenbach, A.; Bickelhaupt, F. M.; Frenking, G. *J. Am. Chem. Soc.* **2000**, *122*, 6449.
- (7) Jonas, V.; Thiele, W. *Organometallics* **1998**, *17*, 353.
- (8) Grinberg, A. A.; Plitsyn, B. V.; Filinov, F. M.; Lavrent'ev, V. N. *Tr. Radiovogo Inst. G. Khlopina, Khim. Geochim.* **1956**, *7*, 14.
- (9) Parry, J.; Carmona, E.; Coles, S.; Hursthouse, M. *J. Am. Chem. Soc.* **1995**, *117*, 2649.
- (10) del Mar Conejo, M.; Parry, J. S.; Carmona, E.; Schultz, M.; Brennann, J. G.; Beshouri, S. M.; Andersen, R. A.; Rogers, R. D.; Coles, S.; Hursthouse, M. *Chem.—Eur. J.* **1999**, *5*, 3000.
- (11) Ricks, A. M.; Gagliardi, L.; Duncan, M. A. *J. Am. Chem. Soc.* **2010**, *132*, 15905.
- (12) Zhou, M.; Andrews, L.; Li, J.; Bursten, B. E. *J. Am. Chem. Soc.* **1999**, *121*, 12188.
- (13) Li, J.; Bursten, B. E.; Zhou, M.; Andrews, L. *Inorg. Chem.* **2001**, *40*, 5448.
- (14) Andrews, L.; Liang, B.; Li, J.; Bursten, B. E. *J. Am. Chem. Soc.* **2003**, *125*, 3126.
- (15) Selg, P.; Brintzinger, H. H.; Schultz, M.; Andersen, R. A. *Organometallics* **2002**, *21*, 3100.
- (16) Maron, L.; Perrin, L.; Eisenstein, O.; Andersen, R. A. *J. Am. Chem. Soc.* **2002**, *124*, 5614.
- (17) Brennan, J. G.; Andersen, R. A.; Robbins, J. L. *J. Am. Chem. Soc.* **1986**, *108*, 335.
- (18) Evans, W. J.; Kozimor, S. A.; Nyce, G. W.; Ziller, J. W. *J. Am. Chem. Soc.* **2003**, *125*, 13831.
- (19) Sheline, R. K.; Slater, J. L. *Angew. Chem., Int. Ed. Engl.* **1975**, *14*, 309.
- (20) Arnold, P. L.; Turner, Z. R.; Bellabarba, R. M.; Tooze, R. P. *Chem. Sci.* **2011**, *2*, 77.
- (21) Mansell, S. M.; Kaltsoyannis, N.; Arnold, P. L. *J. Am. Chem. Soc.* **2011**, *133*, 9036.
- (22) Summerscales, O. T.; Cloke, F. G. N.; Hitchcock, P. B.; Green, J. C.; Hazari, N. *Science* **2006**, *311*, 829.
- (23) Summerscales, O. T.; Cloke, F. G. N.; Hitchcock, P. B.; Green, J. C.; Hazari, N. *J. Am. Chem. Soc.* **2006**, *128*, 9602.
- (24) Frey, A. S.; Cloke, F. G. N.; Hitchcock, P. B.; Day, I. J.; Green, J. C.; Aitken, G. J. *J. Am. Chem. Soc.* **2008**, *130*, 13681.
- (25) Aitken, G.; Hazari, N.; Frey, A. S. P.; Cloke, F. G. N.; Summerscales, O. T.; Green, J. C. *Dalton Trans.* **2011**, *40*, 11080.
- (26) Gardner, B. M.; Stewart, J. C.; Davis, A. L.; McMaster, J.; Lewis, W.; Blake, A. J.; Liddle, S. T. *Proc. Natl. Acad. Sci.* **2012**, *109*, 9265.
- (27) Tsoureas, N.; Summerscales, O. T.; Cloke, F. G. N.; Roe, S. M. *Organometallics* **2013**, *32*, 1353.
- (28) McKay, D.; Frey, A. S. P.; Green, J. C.; Cloke, F. G. N.; Maron, L. *Chem Commun.* **2012**, *48*, 4118.
- (29) Zhang, X.; Li, Q.-S.; Xie, Y.; King, R. B.; Schaefer, H. F. *Inorg. Chem.* **2010**, *49*, 1961.
- (30) Ziegler, T.; Autschbach, J. *Chem. Rev.* **2005**, *105*, 2695.
- (31) Bühl, M.; Kabrede, H. *J. Chem. Theory Comput.* **2006**, *2*, 1282.
- (32) Brynda, M.; Gagliardi, L.; Widmark, P. O.; Power, P. P.; Roos, B. O. *Angew. Chem., Int. Ed.* **2006**, *45*, 3804.
- (33) Sieffert, N.; Bühl, M. *J. Am. Chem. Soc.* **2010**, *132*, 8056.
- (34) Schyman, P.; Lai, W.; Chen, H.; Wang, Y.; Shaik, S. *J. Am. Chem. Soc.* **2011**, *133*, 7977.
- (35) Adams, R. D.; Pearl, W. C.; Wong, Y. O.; Zhang, Q.; Hall, M. B.; Walensky, J. R. *J. Am. Chem. Soc.* **2011**, *133*, 12994.
- (36) Lonsdale, R.; Olah, J.; Mulholland, A. J.; Harvey, J. N. *J. Am. Chem. Soc.* **2011**, *133*, 15464.
- (37) Vlasisavljevich, B.; Gagliardi, L.; Burns, P. C. *J. Am. Chem. Soc.* **2010**, *132*, 14503.

- (38) Shamov, G. A. *J. Am. Chem. Soc.* **2011**, *133*, 4316.
- (39) Cantat, T.; Graves, C. R.; Jantunen, K. C.; Burns, C. J.; Scott, B. L.; Schelter, E. J.; Morris, D. E.; Hay, P. J.; Kiplinger, J. L. *J. Am. Chem. Soc.* **2008**, *130*, 17537.
- (40) Becke, A. D. *Phys. Rev. A* **1988**, *38*, 3098.
- (41) Perdew, J. P. *Phys. Rev. B* **1986**, *33*, 8822.
- (42) Tsipis, A. C.; Kefalidis, C. E.; Tsipis, C. A. *J. Am. Chem. Soc.* **2008**, *130*, 9144.
- (43) Infante, I.; Raab, J.; Lyon, J. T.; Liang, B.; Andrews, L.; Gagliardi, L. *J. Phys. Chem. A* **2007**, *111*, 11996.
- (44) Zhao, Y.; Truhlar, D. G. *J. Chem. Phys.* **2006**, *125*, 194101.
- (45) Zhao, Y.; Truhlar, D. G. *Theor. Chem. Acc.* **2008**, *120*, 215.
- (46) Cao, X.; Dolg, M. *J. Mol. Struct.* **2004**, *673*, 203.
- (47) Schaefer, A.; Horn, H.; Ahlrichs, R. *J. Chem. Phys.* **1992**, *97*, 2571.
- (48) Schaefer, A.; Huber, C.; Ahlrichs, R. *J. Chem. Phys.* **1994**, *100*, 5829.
- (49) Frisch, M. J.; et al. *Gaussian 09*, Revision A.02; Gaussian, Inc.: Wallingford, CT, 2009.
- (50) Papas, B. N.; Schaefer, H. F. *J. Mol. Struct.* **2006**, *768*, 275.
- (51) Sunderlin, L. S.; Wang, D.; Squires, R. R. *J. Am. Chem. Soc.* **1993**, *115*, 12060.
- (52) Weinhold, F.; Landis, C. R. *Valency and Bonding: A Natural Bond Order Donor-Acceptor Perspective*; Cambridge University Press: Cambridge, U. K., 2005; pp 32–36.
- (53) Pyykkö, P.; Atsumi, M. *Chem.—Eur. J.* **2009**, *15*, 12770.
- (54) Popelier, P. *Atoms in Molecules—An Introduction*; UMIST: Manchester, U.K., 2000.
- (55) Matta, C. F., Boyd, R. J., Eds.; *The Quantum Theory of Atoms in Molecules. From Solid State to DNA and Drug Design*; Wiley-VCH: Weinheim, Germany, 2007.
- (56) Lu, T. *Multiwfn: A multifunctional wavefunction analyzer*, Version 2.6.1; 2013; <http://Multiwfn.codeplex.com>.
- (57) Reinhold, J.; Hunstock, E.; Mealli, C. *New J. Chem.* **1994**, *18*, 465.
- (58) Ponec, R.; Lendvay, G.; Chaves, J. *J. Comput. Chem.* **2008**, *29*, 1387.
- (59) Wang, H.; Xie, Y.; King, R. B.; Schaefer, H. F. *J. Am. Chem. Soc.* **2006**, *128*, 11376.
- (60) Bao, X. G.; Zhou, X.; Lovitt, C. F.; Venkatraman, A.; Gleiter, D. A. H.; Hoffmann, R.; Borden, W. T. *J. Am. Chem. Soc.* **2012**, *134*, 10259.
- (61) Liu, X.-M.; Wang, C.-Y.; Li, Q.-S.; Xie, Y.; King, R. B.; Schaefer, H. F. *Chem.—Eur. J.* **2009**, *15*, 5520.
- (62) Gong, X.; Zhang, X.; Li, Q.-S.; Xie, Y.; King, R. B.; Schaefer, H. F. *Dalton Trans.* **2010**, 5242.
- (63) Xu, L.; Li, Q.-S.; King, R. B.; Schaefer, H. F. *Organometallics* **2011**, *30*, 5084.
- (64) Chang, Y.; Li, Q.-S.; Xie, Y.; King, R. B. *Inorg. Chem.* **2012**, *51*, 8904.
- (65) Gagliardi, L.; Roos, B. O. *Nature* **2005**, *433*, 848.
- (66) Roos, B. O.; Malmqvist, P.; Gagliardi, L. *J. Am. Chem. Soc.* **2006**, *128*, 17000.